Available online at www.sciencedirect.com
SCIENCE DIRECT®
International Journal of Thermal Sciences 43 (2004) 1213–1221
International Journal of Thermal Sciences
www.elsevier.com/locate/ijts

Experimental study of convective heat transfer during cooling with low air velocity in a stack of objects

Sami Ben Amara [a,*], Onrawee Laguerre [a], Denis Flick [b]

[a] *Cemagref – Refrigeration Processes Engineering Research Unit, parc de Tourvoie, BP 44, 92163 Antony cedex, France*
[b] *National Agronomic Institute – INAPG, 16 rue Claude Bernard, 75231 Paris cedex 05, France*

Received 4 December 2003; received in revised form 9 April 2004; accepted 9 April 2004

Available online 24 June 2004

Abstract

During cooling with low air velocity ($u \leqslant 0.2\ \mathrm{m{\cdot}s^{-1}}$) of a stack of foodstuffs (a few centimeters dimension), the radiation and conduction between products can be of the same order of magnitude as convection. A method was developed to quantify these various transfer modes. The experiment was carried out using an in-line spherical arrangement; however, the same methodology can be applied to other product shapes. The results confirm that the heat transfers by radiation and conduction cannot be neglected. In addition, the convective heat transfer coefficient varies not only with air velocity but also with the product position in the stack.

Keywords: Convection; Conduction; Radiation; Low air velocity; Stack

1. Introduction

In food industries, during processes such as cooling or drying of a stack of products, quality variations in the final product are often observed according to the position in stack. These heterogeneities are due to the differences in the airflow properties (moisture, temperature, velocity and turbulence) reaching the products. These properties are influenced by several technological parameters (shape of products, spacing, arrangement, packaging, geometry of the air distribution systems).

Many studies have been carried out on forced convection, in particular on the control of the product cooling rate: for oranges [1]; for strawberries [2–4]; for plums and peaches [5,6]; for sweet peppers [7]; for tomatoes [8,9]; for fruit and vegetables [10]; for dairy products [11]. These studies do not take into account heat transfer by conduction and radiation between the products. However, these heat transfer modes cannot be neglected if the convection is carried out using low velocity (particularly in unventilated zones or in equipment inside which heat is transferred by natural convection).

The literature related to heat transfer in porous media and packed beds [12–14] reveal several approaches taking into account various heat transfers modes: conduction, convection and radiation.

The first type of model, called a "one-temperature model", considers that there is a thermal equilibrium between the product and the air (locally, the temperature in the two phases is assumed to be identical).

If the fluid (air in our case) is motionless, the heat transfer by conduction in the medium (solid + fluid) is characterized by effective heat conductivity. This depends on the heat conductivities of the air and the product, the structure of the media (continuous or dispersed), porosity and contact resistance between the products.

If the air flows, the heat transfer is due to both conduction (molecular diffusion) and convection (hydrodynamic mixture of air in pores). The transfer can be characterized in this case by two parameters: the effective heat conductivity and the dispersion coefficient in the air. Several factors can influence this dispersion: porosity, ratio of the voluminal heat capacities of the two phases, ratio of heat conductivities of the two phases, thermal diffusivity and air velocity. The radiation between the surfaces of the particles is also

* Corresponding author. Fax: +33-1-40-96-60-75.
E-mail addresses: sami.benamara@cemagref.fr (S. Ben Amara), onrawee.laguerre@cemagref.fr (O. Laguerre), flick@inapg.inra.fr (D. Flick).

1290-0729/$ – see front matter
doi:10.1016/j.ijthermalsci.2004.04.004

Nomenclature

A	heat transfer surface	m^2
a_v	specific surface; ratio between surface of object and volume of the bed occupied by these objects	m^{-1}
Bi	Biot number, $= h \cdot R \cdot \lambda_p^{-1}$	
C	contact conductance between 2 spheres	$W{\cdot}K^{-1}$
C'	equivalent conductance by radiation between 2 spheres	$W{\cdot}K^{-1}$
Cp	air specific heat	$J{\cdot}kg^{-1}{\cdot}K^{-1}$
Cp_p	product specific heat	$J{\cdot}kg^{-1}{\cdot}K^{-1}$
D	sphere diameter	m
Gr	Grashof number, $= g \cdot \beta \cdot D^3 \cdot (T_{h.s} - T_{\text{air}}) \cdot \nu^{-2}$	
g	gravitational acceleration	$m{\cdot}s^{-2}$
h	convective heat transfer coefficient based on upstream air temperature	$W{\cdot}m^{-2}{\cdot}K^{-1}$
h'	convective heat transfer coefficient based on mean air temperature	$W{\cdot}m^{-2}{\cdot}K^{-1}$
m	sphere weight	kg
$\dot{m}$	air mass flow rate over a cross section of D^2	$m{\cdot}s^{-1}$
Nu	Nusselt number, $= h \cdot D \cdot \lambda^{-1}$	
Pr	Prandtl number, $Pr = \mu \cdot Cp \cdot \lambda^{-1}$, $Pr = 0.71$ for air	
$\dot{Q}$	heating power	W
R	sphere radius	m
R_h	heating resistance	Ω
Re	Reynolds number, $= \rho \cdot u \cdot D \cdot \mu^{-1}$	
T_{air}	inlet air temperature on the stacking	K
T_m	average product temperature (average value between $T_{h.s}$ and $T_{s.1}$)	K
T_p	product temperature	K
$T_{s.1}$	temperature of the hollow celluloid sphere in contact with the heating sphere	K
$T_{s.2}$	temperature of the black hollow celluloid sphere in contact with the receiving sphere	K
$T_{h.s}$	heating brass sphere temperature	K
$T_{r.s}$	receiving brass sphere temperature	K
$T\{x, y\}$	sphere temperature centred in $\{x, y\}$	K
u	air velocity at the entrance of the stack	$m{\cdot}s^{-1}$
U	heating voltage	V

Greek symbol

β	thermal expansion coefficient	K^{-1}
ΔP	pressure drop	Pa
ΔP_m	mean difference between upstream and downstream air temperature	K
ε	emissivity	
Φ_{rad}	radiation heat flux	$W{\cdot}m^{-2}{\cdot}K^{-1}$
λ	air thermal conductivity	$W{\cdot}m^{-1}{\cdot}K^{-1}$
λ_e	equivalent thermal conductivity	$W{\cdot}m^{-1}{\cdot}K^{-1}$
λ_{ef}	equivalent thermal conductivity in the fluid phase	$W{\cdot}m^{-1}{\cdot}K^{-1}$
λ_{es}	equivalent thermal conductivity in the solid phase	$W{\cdot}m^{-1}{\cdot}K^{-1}$
λ_p	product thermal conductivity	$W{\cdot}m^{-1}{\cdot}K^{-1}$
μ	air dynamic viscosity	Pa s
ν	air kinematic viscosity	$m^2{\cdot}s^{-1}$
ρ	air density	$kg{\cdot}m^{-3}$
ρ_p	product density	$kg{\cdot}m^{-3}$
σ	Stefan–Boltzmann constant, $= 5.67040 \times 10^{-8}$	$W{\cdot}m^{-2}{\cdot}K^{-4}$

important and should be taken into account, particularly at high temperatures. This influence has been less investigated in porous media compared with conduction and convection. This transfer mode can be approached using radiative conductivity, which depends primarily on the emissivity of surfaces and the geometry of the pores (which influences the view factor).

Several authors proposed empirical correlations making it possible to estimate these parameters: effective heat conductivity (contact between two spheres [14]; contact between two cylinders [15]), dispersion coefficient in spheres in bulk [16,17] and radiative conductivity (two flat plates [18]; periodically arranged spheres [14]).

The "one-temperature model" cannot be applied in certain circumstances, particularly in the transient state. The model called the "two-temperature model" where, locally, each phase is represented by a temperature, is then often used. The simplest and the least precise two-temperature model is that of Schumann [19] which takes into account only the convection between air and particles.

A more sophisticated model, called the "continuous solid model" takes into account conduction by using 2 parameters: effective heat conductivities of the solid phase (λ_{es}) and the fluid phase (λ_{ef}).

Lastly, the model called "dispersed-particle-based model" is more complex than the preceding one. It takes into account conduction within each particle by locally introducing a continuous temperature variation between the center and the surface of product. This model also takes into account conduction and dispersion in the air; while at the surface of the particles, the exchange takes place only through convection.

All these models require experimental identification of the parameters, which is, in general, obtained indirectly by fluid temperature measurements.

This work directly analyses the heat exchanges between the product and the air by imposing heat sources and by measuring the product and the air temperatures. Quantification of heat transfer by convection, conduction and radiation was performed. The results make it possible to explain and

quantify the effect of various factors (air velocity, position, air-product temperature difference) on the transfers during cooling with a low air velocity ($u < 0.2$ m·s^{-1}), of a stack of products.

To simplify the phenomena, as a first approach, the following conditions were used:

- A simple geometry (in-line stack of spheres, one-directional flow).
- No mass transfer due to water evaporation occurs at the surface of the products.
- The internal heat transfer resistance of the particles was low in our experiment (high thermal conductivity spheres).

Since the final objective of this study is to reduce the heterogeneities of treatment in food industry, a more complex geometry, evaporation and internal heat transfer resistance should be taken into account to better reflect the characteristics of foods.

2. Materials and methods

2.1. Experimental device

The experimental device is composed of an open PVC cavity (cross section 0.19 m × 0.19 m). It can contain up to 10 rows (in-line arrangement) of hollow celluloid spheres (∅38 × 10^{-3} m) and each row contains 5 × 5 spheres (Fig. 1(a)). The device is located in a controlled temperature room. An unidirectional airflow (from top to bottom of the stack) is achieved by suction with a blower. Air velocity is regulated using a frequency variator; velocity can vary from 0.03 to 0.20 m·s^{-1}. The airflow rate is measured by means of an Annubar probe. A differential pressure sensor (Differential Presses Transmitter Model FCO352) is used to measure the pressure drop in the stack (precision ±0.25%). The air temperature at the entrance of the cavity is measured using calibrated thermocouples (type T). All the measuring instruments are connected to a data logger (FLUKE HELIOS I).

2.2. Methods

The heat transfer coefficient is measured in steady state regime using an instrumented brass sphere equipped with a thermocouple (type T) and a heating wire (Fig. 1(b)). Then this sphere is introduced at various positions inside the stack. The heat exchanges by convection, radiation and conduction were quantified using different types of spheres:

- Hollow white celluloid spheres (very low conductivity).
- Black painted hollow celluloid spheres (very low conductivity, high emissivity).

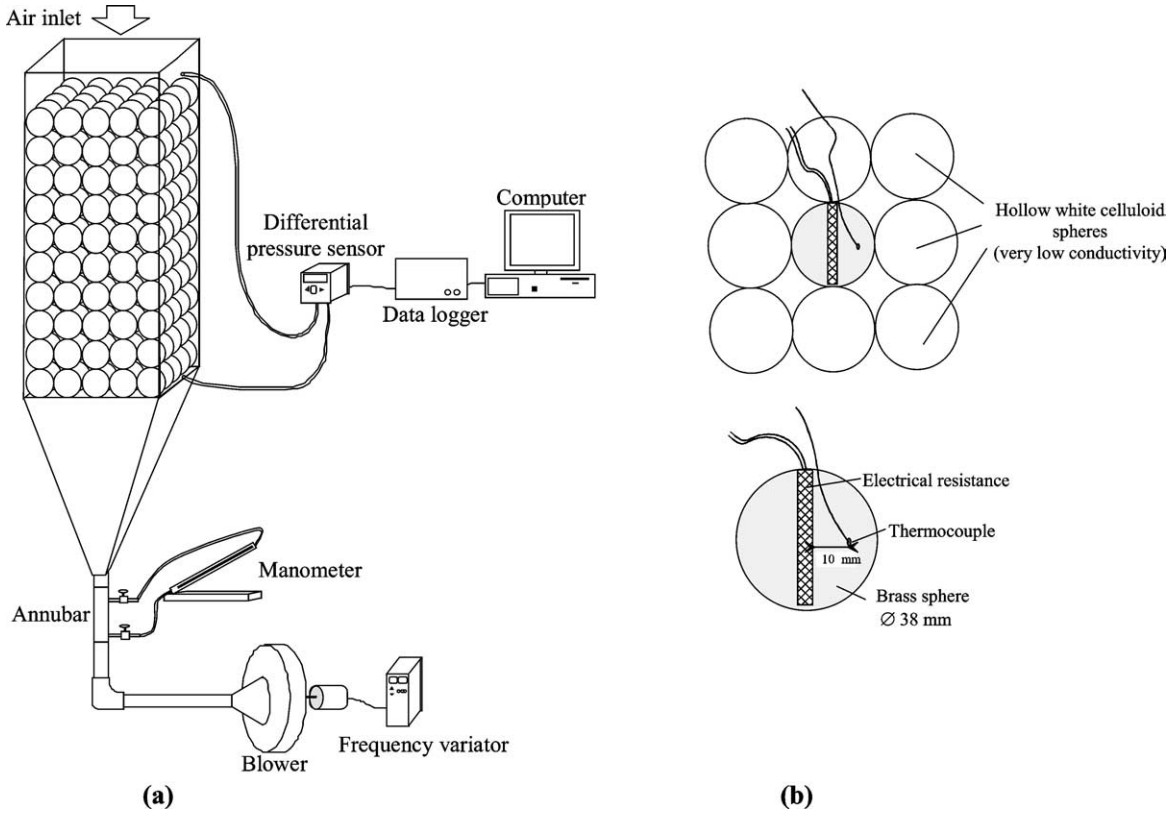

Fig. 1. (a) Experimental device; (b) Spherical sensor used for the measurement of the heat transfer coefficient.

– Chromed brass spheres (high conductivity, low emissivity; $\varepsilon = 0.12$).
– Black painted brass spheres (high conductivity, high emissivity; $\varepsilon = 0.97$).

Four experiments were carried out to distinguish the effects of the various transfer modes (Fig. 2):

(a) Characterization of the pure convection by introducing a chromed brass-heating sphere (low emissivity) in the stack that contains white celluloid hollow spheres. Thus, heat transfer by conduction and radiation is limited.
(b) Characterization of the combined convection and conduction by introducing a chromed brass-heating sphere in the stack of hollow white celluloid spheres. Another "receiving" chromed brass sphere (simply equipped with a thermocouple), is placed near the heated one. In this manner, heat transfer by conduction due to the contact between these two spheres is promoted but radiation is limited.
(c) Characterization of the combined convection and radiation by introducing a black painted heating brass sphere (high emissivity) into a stacking of black painted hollow celluloid spheres. Thus, heat transfer by conduction between spheres is limited, but radiation occurs.
(d) Characterization of the convection, conduction and radiation by introducing two black painted brass spheres (a heated and a receiving one) in the stack of black painted hollow celluloid spheres. Thus, all heat transfer modes are promoted. This experiment was used to validate the results obtained in (a), (b) and (c).

It should be noted that the four experiments were carried out under the same conditions; the inlet air velocity was set at 0.11 $\mathrm{m{\cdot}s^{-1}}$ and the heated brass sphere was placed in the middle of the 5th row of the 10-row stack. In addition, the heating power is adjusted so that the temperature difference between the heating sphere and the inlet air was set at 15 ± 0.2 K.

Then, the influence of the position of the heating sphere in the stack, the inlet air velocity and the temperature difference between the heating sphere and the air on convection were explored. The second types of experiments were carried out by placing the heated chromed brass sphere in the stack of hollow white celluloid spheres (limited conduction and radiation).

2.3. Characterization of convection (Fig. 2(a))

The convective heat transfer coefficient is measured in steady state [20] by neglecting conduction between spheres (hollow celluloid spheres) and radiation (chromed brass sphere).

A homogeneous temperature of the heating sphere can be assumed. Indeed, the heat conductivity of brass is high ($\lambda_{\mathrm{brass}} = 126$ $\mathrm{W{\cdot}m{\cdot}K^{-1}}$) and the convective heat transfer

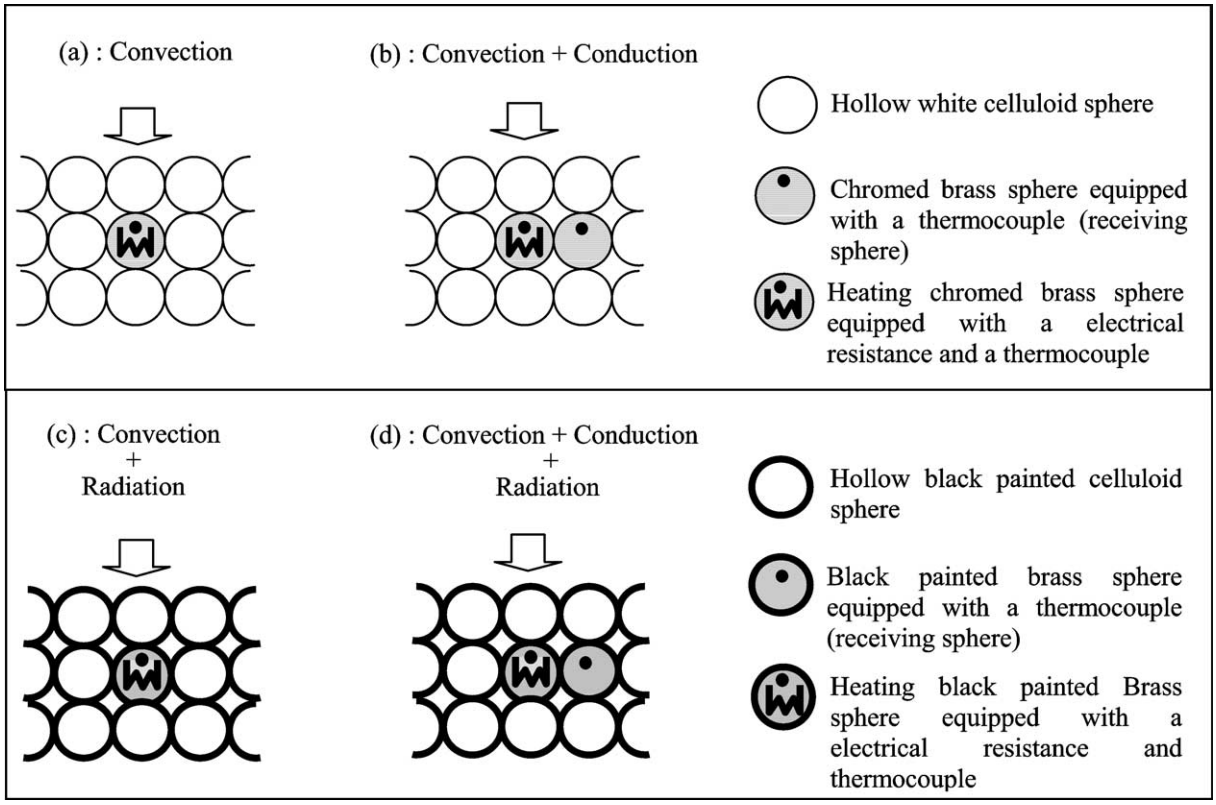

Fig. 2. Four experiments used to quantify convection, conduction and radiation.

coefficient was less than 14 $W \cdot m \cdot K^{-1}$ in our experiments; therefore the Biot number is always less than 2×10^{-3}. The convective heat transfer coefficient was defined by the following equation:

$$h = \frac{\dot{Q}}{A(T_{h.s} - T_{\text{air}})} \tag{1}$$

$$\dot{Q} = \frac{U^2}{R_h} \tag{2}$$

2.4. Characterization of convection and conduction (Fig. 2(b))

The steady state heat balance for the heated and the receiving chromed brass spheres was developed as follows:

For the heating sphere:

$$\dot{Q} + hA(T_{\text{air}} - T_{h.s}) + C(T_{r.s} - T_{h.s}) = 0 \tag{3}$$

For the receiving sphere:

$$hA(T_{\text{air}} - T_{r.s}) + C(T_{h.s} - T_{r.s}) = 0 \tag{4}$$

Where C is the contact conductance between the two spheres. Knowing the experimental values of $\dot{Q}$, $T_{h.s}$, $T_{r.s}$ and T_{air}, the values of h and C can be calculated.

2.5. Characterizations of convection and radiation (Fig. 2(c))

The heat balance on black painted heated brass sphere and on black painted hollow celluloid sphere was developed as follows:

For the black painted heating brass sphere:

$$\dot{Q} + hA(T_{\text{air}} - T_{h.s}) + 6C'(T_{s.1} - T_{h.s}) = 0 \tag{5}$$

It is considered here that, in addition to convection between the heating sphere and the surrounding air, there is also radiation between this sphere and the 6 neighbouring ones (the experimental device being three-dimensional). The C' coefficient represent the equivalent conductance due to the exchange by radiation between these spheres. This exchange is normally proportional to $(T_{s.1}^4 - T_{h.s}^4)$, since $(T_{h.s} - T_{s.1}) \ll (T_{h.s} + T_{s.1})$, a linearization is possible.

For the black painted hollow celluloid sphere:

$$h\frac{A}{2}(T_{\text{air}} - T_{s.1}) + C'(T_{h.s} - T_{s.1}) = 0 \tag{6}$$

It is considered that a half of the hollow celluloid sphere surface (which is in contact with the heating sphere) receives radiative heat and this is evacuated by convection on this same surface (conduction within the hollow celluloid sphere is neglected).

C' and $T_{s.1}$ values can be calculated knowing the experimental values of $\dot{Q}$, $T_{h.s}$, T_{air} and using the value of h obtained from the pure convection experiment (same experimental conditions: position in the stack, air velocity, temperature difference between $T_{h.s}$ and T_{air}).

2.6. Characterization of convection, conduction and radiation (Fig. 2(d))

This experiment, which combines all transfer modes, was used here for validation. By applying the values of h, C and C' obtained from preceding experiments, values of $T_{h.s}$ and $T_{r.s}$ can be calculated (from $\dot{Q}$ and T_{air}) and compared with the experimental ones.

Heat balance on the heating sphere:

$$\dot{Q} + hA(T_{\text{air}} - T_{h.s}) + C(T_{r.s} - T_{h.s}) + 5C'(T_{s.1} - T_{h.s}) + C'(T_{r.s} - T_{h.s}) = 0 \tag{7}$$

Heat balance on the receiving sphere:

$$hA(T_{\text{air}} - T_{r.s}) + C(T_{h.s} - T_{r.s}) + 5C'(T_{s.2} - T_{r.s}) + C'(T_{h.s} - T_{r.s}) = 0 \tag{8}$$

Heat balance on a hollow celluloid sphere in contact with the heating sphere:

$$h\frac{A}{2}(T_{\text{air}} - T_{s.1}) + C'(T_{h.s} - T_{s.1}) = 0 \tag{9}$$

Heat balance on a hollow celluloid sphere in contact with the receiving sphere:

$$h\frac{A}{2}(T_{\text{air}} - T_{s.2}) + C'(T_{r.s} - T_{s.2}) = 0 \tag{10}$$

3. Results

3.1. Estimation of heat transfer coefficient by convection, conduction and radiation

The comparison of the values of C, C' and $h \times A$, presented in Table 1, shows that the transfers by radiation and conduction are of the same order of magnitude as that by convection and cannot be neglected at low air velocity. It can be noted that the heating power required to maintain a 15 K difference between the heating sphere and the air increase with the number of heat transfer modes. The combined transfer by convection and radiation, for example, consumes 39% more power than that in the case of pure convection.

The conductance C depends on the heat conductivity of the brass sphere, the heat conductivity of the air and that of the spheres in the stack. The C value is used to estimate the equivalent conductivity of the porous media (λ_e). It will be shown below that $C = \lambda_e \times D$. Wakao and Kaguei [14] proposed a correlation representing λ_e in the case of unidirectional heat transfer by conduction between two spheres:

$$\frac{\lambda_e}{\lambda} = \frac{2}{1 - \lambda/\lambda_p}\left(\frac{\ln(\lambda_p/\lambda)}{1 - \lambda/\lambda_p} - 1\right) \tag{11}$$

The C value calculated by this correlation is equal to 1.46×10^{-2} $W \cdot K^{-1}$ which is rather different from that of the experimental one (but same order of magnitude $C \approx 2.56 \times$

Table 1
Characterization of the various modes of transfer (middle of the 5th row; $u = 0.11$ m·s^{-1}; $(T_{h.s} - T_{\text{air}}) = 15$ K)

	Convection	Convection + Conduction	Convection + Radiation
$\dot{Q}$ [W]	0.95	1.19	1.33
Increase in power compared to the case pure convection	–	+25%	+39%
h [W·m^{-2}·K^{-1}]	13.94	13.61	13.94
$h \times A$ [W·K^{-1}]	6.32×10^{-2}	6.17×10^{-2}	6.32×10^{-2}
C [W·K^{-1}]	–	2.56×10^{-2}	–
C' [W·K^{-1}]	–	–	4.81×10^{-3}

10^{-2} W·K^{-1}). The flux lines proposed by the correlation are unidirectional and parallel, but this hypothesis is not verified in reality since the flux lines are converged through the contact point between two spheres. Nevertheless, our result can be expressed in the form of a dimensionless number, which can be applied to other diameters (for in-line sphere arrangement and for $\lambda_p/\lambda = 4.9 \times 10^3$):

$$\frac{\lambda_e}{\lambda} = \frac{C}{\lambda D} \approx 26.3 \tag{12}$$

In a similar way, it can be noted that the equivalent conductance by radiation C' is a function of emissivity and arrangement. Wakao and Kaguei [14] proposed an approximation of radiative flow in a porous medium according to the average product temperature T_m (on the basis of the radiative heat balance between large grey surfaces):

$$\Phi_{\text{rad}} = \frac{4\sigma T_m^3}{2/\varepsilon - 1}(T_{s.1} - T_{h.s}) \tag{13}$$

According to this relation, the equivalent conductance by radiation can be expressed as follows:

$$C' = \frac{4\sigma T_m^3}{2/\varepsilon - 1} D^2 \tag{14}$$

The C' value calculated using this correlation is equal to 8.41×10^{-3} W·K^{-1} which is relatively different from that of the experimental one ($C' \approx 4.81 \times 10^{-3}$ W·K^{-1}). The correlation is developed for heat exchange by radiation between two parallel plates, but it consists of two hemispheres in our case. Nevertheless, our result can be expressed in the form of a dimensionless number (for an in-line sphere arrangement and $\varepsilon = 0.97$):

$$\frac{C'}{D^2 \sigma T_m^3} \approx 2.15 \tag{15}$$

The last experiment was used for the validation (Fig. 2(d)). Table 2 compares the calculated and measured temperature of the heating sphere and receiving sphere. It can be seen that calculation slightly underestimates the temperature of the heating sphere and overestimates the temperature of the receiving sphere. This difference could be due to the approximation in Eqs. (9) and (10) in which we supposed that only a half of the surface of the hollow black painted celluloid spheres participate in radiation.

Table 2
Comparison of the temperatures of heating sphere ($T_{h.s}$) and receiving sphere ($T_{r.s}$) estimated and measured for the last experiment

	$T_{h.s}$ [K]	$T_{r.s}$ [K]
Measured	308.0	295.6
Calculated	306.2	296.5

It could be also explained by contact problems between the heating sphere and the receiving one. Indeed, if the contact between the two spheres is not punctual, there will be fine air layer between these two spheres, which may cause variations in conductance by contact C (Table 1).

3.2. Influence of the operating parameters on the convective heat transfer coefficient

Three experiments were carried out to study the influence of the operating parameters on the convective heat transfer coefficient.

In the first experiment, the influence of the temperature difference (between the heating sphere and the air) on the convective heat transfer coefficient was studied for three inlet air velocities (0.11, 0.05 and 0.03 m·s^{-1}). The temperature difference varied from 2.3 to 43.1 K. The chromed brass-heating sphere is placed in the middle of the 5th row of the 10-row stack. It is observed that the estimated convective heat transfer coefficient is independent of the temperature difference between the heating sphere and the air (Fig. 3). However, it should be noted that in our experiments, the Grashof number is lower than 3×10^5 whereas the Reynolds number is always higher than 70. For a higher ($Gr \cdot Re^{-2}$) ratio, an effect of localized natural convection around a hot object is, nevertheless, possible [13].

In the second experiment, the influence of the heating sphere position in stacking on the convective heat transfer coefficient was studied for three inlet air velocities (0.11, 0.05 and 0.03 m·s^{-1}). The temperature difference between the heating sphere and the air was set at 15 ± 0.2 K.

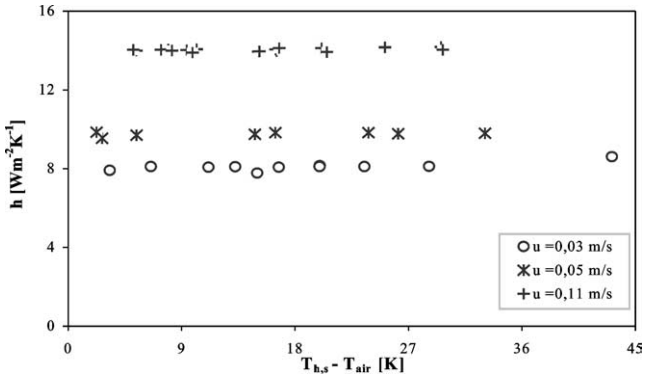

Fig. 3. Influence of the temperature difference between the heating sphere and the air on the convective heat transfer coefficient (sensor placed in the middle of the 5th row).

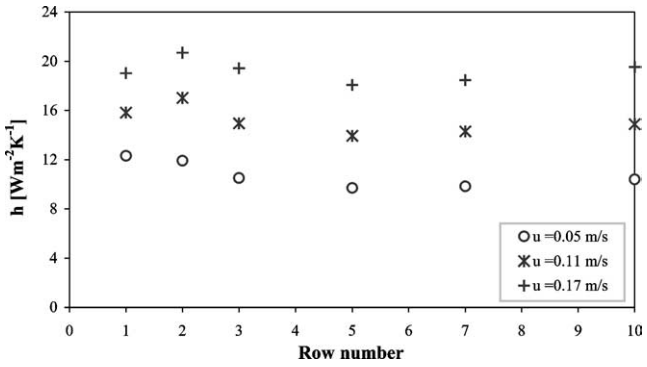

Fig. 4. Influence of the product position in the stack on the convective heat transfer coefficient ($T_{h.s} - T_{\text{air}} = 15$ K).

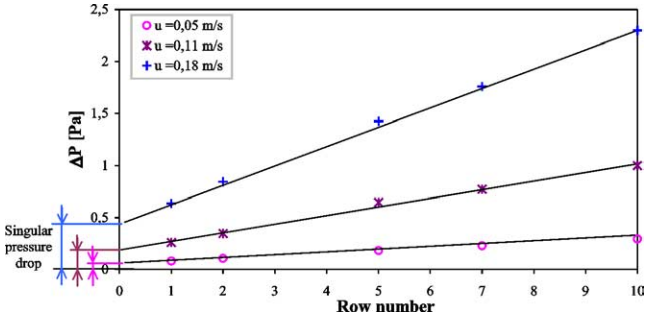

Fig. 5. Influence of the number of rows on the pressure drop in the stack.

It is observed (Fig. 4) that the heat transfer intensifies on the two first and on the last row. This is certainly due to the effects of abrupt reduction and expansion of air passage at the inlet and outlet of the stack. In the central zone of the stack (from the 4th to the 9th rows), the airflow is fully developed; thus, the convective heat transfer coefficient is relatively constant. The increase in the transfer coefficient in the entrance and exit areas can be related to the aerodynamic results. This reveals that the pressure drop is not only proportional to the depth of the bed, but also depends on a singular pressure drop related to the effects of abrupt reduction and expansion at the inlet and outlet of the bed (Fig. 5). In food stacks, product dimensions are often of

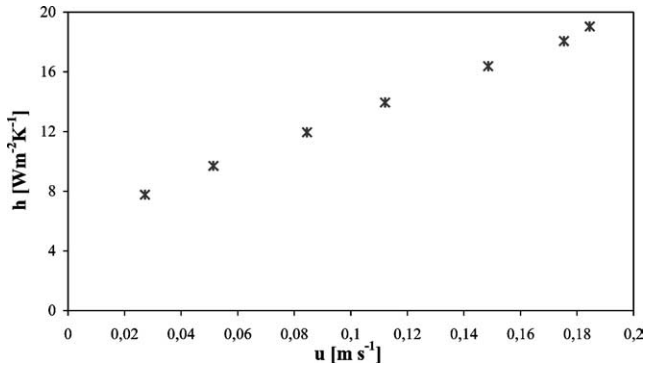

Fig. 6. Influence of the air velocity on the convective heat transfer coefficient (sensor placed in the middle of the 5th row, ($T_{h.s} - T_{\text{air}}) = 15$ K).

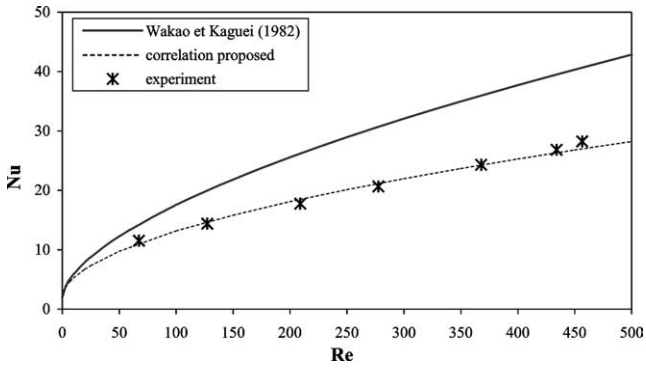

Fig. 7. Influence of the air velocity on the convective heat transfer: comparison with the correlation suggested by Wakao and Kaguei (1982).

the same order of magnitude as those of the container. The phenomena observed at the entrance and exit cannot be neglected and explain part of the product temperature heterogeneity.

In the third experiment, the influence of the air velocity on the convective heat transfer coefficient was quantified (Fig. 6). The temperature difference between the heating sphere and the air is fixed at 15 ± 0.2 K. The heating sphere was placed in the middle of the 5th row of a 10-row stack. The air velocity varied from 0.03 to 0.18 $\text{m}\cdot\text{s}^{-1}$.

For a bulk stack of spheres, Wakao and Kaguei [14] proposed the following correlation between the Nusselt number and the Reynolds number ($3 < Re < 3000$)

$$Nu = 1.10\,Pr^{1/3}Re^{0.60} + 2 \tag{16}$$

Since the Reynolds number ranged from 74 to 495 in our experiment, we propose a similar correlation in which the coefficients, identified by adjustment of the experimental results, are close to those proposed by Wakao and Kaguei [14]:

$$Nu = 1.09\,Pr^{1/3}Re^{0.53} + 2 \tag{17}$$

The difference observed (Fig. 7) between the two correlations can be explained by the fact that, in our case, the periodic sphere arrangement contributes to both channeling and unventilated zones. This phenomenon is not often observed in bulk stacking.

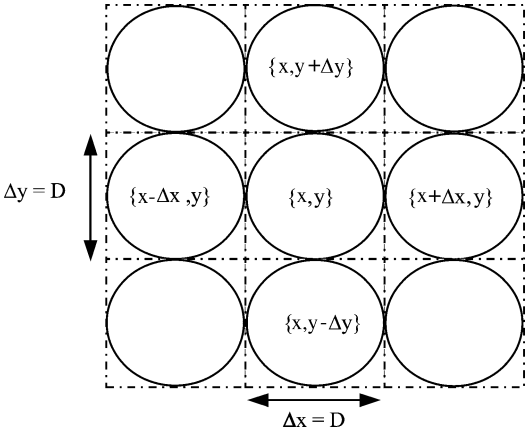

Fig. 8. Two-dimensional Cartesian grid.

3.3. Modeling of heat transfer in a stack of products

The results obtained previously (convective heat transfer coefficient vs. velocity and position, conductance due to contact and equivalent conductance due to radiation) can be used to develop a two-temperature heat transfer model in a regular product stack.

The equations of heat balance on the spheres can be considered as the discretized form of partial derivative equations (PDE) as shown below and these PDE equations are proposed to be used thereafter in an empirical manner for bulk stacking of foodstuffs. In spite of the fact that this approach is not as rigorous as homogenization methods [21,22], it leads to formally similar relations and makes it possible to link the concepts of conductance C and C' to those of effective conductivity of the solid phase.

Given a regular stack (as in our experiments) and a Cartesian grid (two-dimensional to simplify the writing up) with space step equal to the diameter of the spheres (Fig. 8), the heat balance of one sphere can be written as follows:

$$\begin{aligned} mCp_p \frac{\mathrm{d}T_p\{x,y\}}{\mathrm{d}t} &= hA\big(T_{\mathrm{air}}\{x,y\} - T_p\{x,y\}\big) \\ &\quad + \big(C + C'\big)\big[T_p\{x+\Delta x,y\} - T_p\{x,y\} \\ &\quad + T_p\{x-\Delta x,y\} - T_p\{x,y\} + T_p\{x,y+\Delta y\} \\ &\quad - T_p\{x,y\} + T_p\{x,y-\Delta y\} - T_p\{x,y\}\big] \end{aligned} \tag{18}$$

where $m = \rho_p D^3(1-\varepsilon)$, $A = a_V D^3$, $a_V = \pi/D$ and $\{x, y\}$ is the coordinate of the sphere center.

This equation can be represented in a PDE form:

$$(1-\varepsilon)\rho_p Cp_p \frac{\partial T_p}{\partial t} = \vec{\nabla}\cdot\big(\lambda_{\mathrm{es}}\vec{\nabla}T_p\big) + ha_V(T_{\mathrm{air}} - T_p) \tag{19}$$

where $\lambda_{\mathrm{es}} = (C + C')/D$.

The heat balance on air can be obtained in the same manner:

$$\rho Cp\left[\varepsilon\frac{\partial T_{\mathrm{air}}}{\partial t} + \vec{u}\cdot\vec{\nabla}T_{\mathrm{air}}\right] = \vec{\nabla}\cdot\big(\lambda_{\mathrm{ef}}\vec{\nabla}T_p\big) + ha_V(T_p - T_{\mathrm{air}}) \tag{20}$$

The prediction of the equivalent conductivity tensor in air is not possible using our study, since it takes into account molecular conduction and aerodynamic dispersion simultaneously; some correlations are proposed by Wakao and Kaguei [14].

It should be noted that T_{air} (Eqs. (18)–(20)) represents the average temperature of the air in the mesh which surrounds a sphere, whereas, the upstream air temperature was used to estimate experimental convective heat transfer coefficient (the upstream temperature of the heating sphere is equal to the air temperature at the inlet of the stack because the temperature increase due to the friction in the stack is negligible). A correction is nevertheless possible. By neglecting the diffusion in the air and the heat exchanges by conduction and radiation with the neighbouring spheres, the temperature difference between upstream and downstream of one sphere is:

$$\Delta T_m = \frac{\dot{Q}}{\dot{m}\,Cp} = \frac{\pi h(T_{h.s} - T_{\mathrm{air}})}{\rho u\,Cp} \tag{21}$$

The convective heat transfer coefficient in which the mean between upstream and downstream air temperature is used, h' can be expressed as:

$$h'(u) = h(u)\cdot\left[1 - \frac{\pi h(u)}{2\rho u\,Cp}\right]^{-1} \tag{22}$$

h is the measured convective heat transfer coefficient in which the air upstream is used.

The correction term in Eq. (22) (correction term $= \pi h(u) \times (2\rho u\,Cp)^{-1}$) can be omitted for high air velocity (forced convection) but not for low air velocity (natural convection).

4. Conclusion

The experimental results showed that, during heat treatment using low air velocity of a stack of objects (with a size comparable to that of foodstuffs), the various transfer modes (convection, conduction and radiation) are of the same order of magnitude and none of them can be neglected. The convective heat transfer coefficient is a function of air velocity and product position in the stack. The influence of the product position is certainly related to the abrupt reduction and expansion of air passage at the entry and the exit of the stack. The heat balance equations relating to an object, its neighbour and the surrounding air were developed in the form of partial derivative equations. These equations could be applied to any bulk arrangement of products (if the model parameters are estimated for the specific product shape and arrangement) to predict heat transfer and improve their homogeneity in industrial situations.

Acknowledgements

The authors would like to thank to the French Ministry of Agriculture and the "Ile de France Regional Council" for their financial support.

References

[1] C.D. Baird, J.J. Gaffney, D.T. Kinard, Research facility for forced air precooling of fruits and vegetables, ASHRAE Trans. 94 (1975) 1434–1454.
[2] B.B. Arifin, K.V. Chau, Forced-air cooling of strawberries, ASAE, 1987, Paper No 87-6004.
[3] B.B. Arifin, K.V. Chau, Cooling of strawberries in cartons with new vent hole designs, ASHRAE Trans. 94 (1988) 1415–1426.
[4] J.P. Emond, F. Mercier, S.O. Sadfa, M. Bourre, A. Gakwaya, Study parameters affecting cooling rate and temperature distribution in forced air precooling of strawberries, Trans. ASAE 39 (1996) 2185–2191.
[5] N.D. Amos, D.J. Cleland, N.H. Banks, Effect of pallet stacking arrangement on fruit cooling rates within forced air pre-coolers, in: IIF/IIR-Commissions B-B2-D1-D2/3, Palmerston North, New Zealand, 1993, pp. 232–241.
[6] R.A. Parsons, F.G. Mitchell, G. Mayer, Forced air cooling in palletised fresh fruit, Trans. ASAE (1970), Paper No 70-875.
[7] J.J. Gaffney, C.D. Bird, Forced air cooling of bell peppers in bulk, Trans. ASAE (1977) 1174–1977.
[8] J.K. Wang, K. Tupun, Forced air precooling of tomatoes in carton, Trans. ASAE (1969) 804–806.
[9] A.H. Bennett, H.L. Strum, A. Aharoni, A velocity type forced-air vegetable precooler, ASHRAE J. 12 (1980) 23–27.
[10] G. Alvarez, D. Flick, Analysis of heterogeneous cooling of agricultural products inside bins. Part I: Aerodynamic study, J. Food Engrg. 39 (1999) 227–237.
[11] N. Carniol, Transfert convectifs de chaleur dans les ensembles réguliers de produits alimentaires, Ph.D. Thesis, Ecole Nationale Supérieure des Industries Agricoles et Alimentaires ENSIA-MASSY, France, 2000.
[12] J. Padet, Principes des Transferts Convectif, Polytechnica, Paris, 1997.
[13] W. Rohsenow, J. Hartnett, Y. Cho, Handbook of Heat Transfer, McGraw-Hill, New York, 1998.
[14] N. Wakao, S. Kaguei, Heat and Mass Transfer in Packed Beds, Gordon and Breach, New York, 1982.
[15] R. Krupiczka, Analysis of heat conductivity in granular materials, Internat. Chem. Engrg. (1967) 122–144.
[16] G. De Josselin De Jong, Longitudinal and transverse diffusion in granular deposits, Trans. Amer. Geophys. Union 39 (1958) 67–74.
[17] D.L. Koch, J.F. Brady, Dispersion in fixed beds, J. Fluid Mech. 154 (1985) 399–427.
[18] C.L. Tien, B.L. Drolen, Heat radiation in particulate media with dependent and independent dispersioning, Annual Rev. Numer. Fluid Mech. Heat Transfer 1 (1987) 1–32.
[19] T.E.W. Schumann, Heat transfer: A liquid flowing through a porous prism, J. Franklin Inst. 208 (1962) 405–416.
[20] G. Alvarez, D. Flick, Analysis of heterogeneous cooling of agricultural products inside bins. Part II: Thermal study, J. Food Engrg. 39 (1999) 239–245.
[21] M. Quintard, S. Whitaker, Transport in ordered and disordered porous media I: The cellular average and the use of weighting functions, Transport in Porous Media 14 (1994) 163–177.
[22] M. Quintard, S. Whitaker, Transport in ordered and disordered porous media II: Generalized volume averaging, Transport in Porous Media 14 (1994) 179–206.